

Patterns and localized structures in bistable semiconductor resonators

V.B.Taranenko, I.Ganne,* R.J.Kuszelewicz,* C.O.Weiss
Physikalisch-Technische Bundesanstalt 38116 Braunschweig/Germany
**Centre National d'Etudes de Telecommunication, Bagneux/France*

We report experiments on spatial switching dynamics and steady state structures of passive nonlinear semiconductor resonators of large Fresnel number. Extended patterns and switching front dynamics are observed and investigated. Evidence of localization of structures is given.

PACS 42.65.Sf; 42.65.Tg; 42.70.Nq

It has recently become apparent that pattern formation in optics is related in many ways with other fields of physics [1]. One simple optical pattern forming system is a nonlinear resonator, the subject of recent investigations see, e.g. [2] and op.cit. The analogy of resonator optics with fluids [3], particularly, suggests a variety of phenomena not considered for optics before [4]. For active resonators (lasers, lasers with nonlinear absorber, 4-wave mixing oscillators) predicted phenomena, such as vortices and spatial solitons, have already been demonstrated experimentally [2]. On the other hand, experimental results for passive resonators, recently studied extensively theoretically with a view to possible application [5,6], are limited to the early demonstration of structures in resonators containing liquid crystals or alkali vapours as the nonlinear medium [7]. We report here the first experimental investigations of structure formation in passive nonlinear semiconductor resonators. These systems, apart from possible usefulness in applications, show phenomena in optics analogous to those found in other fields of nonlinear physics (e.g. optical Turing instability [8] or competition between pattern formation and switching [9]). Our observations include regular (hexagonal) pattern formation and, in presence of optical bistability (OB), space- and time-resolved switching waves. We also present observations which indicate mutual locking of OB switching waves to form localized structures (spatial solitons) [15]. Further evidence of localization effects is shown by independently switch bright spots of a hexagonal structure.

The resonator used for the experiment consists of GaAs/GaAlAs multiple quantum well (MQW) material (18 periods of GaAs/Ga_{0.5}Al_{0.5}As with 10 nm/10 nm thickness) between Bragg mirrors of about 99.5 % reflectivity on a GaAs substrate. Properties of these microresonators have been described in [10]. The optical resonator length is approximately 3 μm with a corresponding free spectral range of 50 THz. The resonator thickness varies over the usable sample area (10 x 20 mm). So, by choosing a particular position on the sample, it is possible to vary the cavity resonance wavelength such that its downshift $\Delta\lambda$ below the exciton line lies in the range $0 < \Delta\lambda < 25 \text{ nm}$.

The absorption of the MQW material depends on $\Delta\lambda$. A typical finesse of the resonator far below the exciton energy is 200, which corresponds to 125 GHz half width at half maximum (HWHM) of the cavity resonance.

The radiation source used is a continuous-wave Ar⁺-pumped Ti:Al₂O₃-laser. To realize a reasonable Fresnel number, the radiation has a spot width on the sample of about 60 μm . The nonlinearity used is predominantly dispersive and defocusing. The characteristic (bistable/monostable) and shape of the resonator response depends on both $\Delta\lambda$ and the detuning $\delta\lambda$ of the laser field from the resonator resonance.

As the substrate for the resonator is opaque, all observations are done in reflection. The OB describing the reflection returned from the input surface is "N-shaped" [10], and complementary to the intracavity field characteristic, which has the familiar "S-shape". To avoid confusion, we will therefore refer to "switched" and "unswitched", rather than "upper" and "lower", states.

Within the illuminated area, smaller areas ($\approx 8 \mu\text{m}$) can be irradiated by short pulses ($\leq 0.1 \mu\text{s}$) to initiate local switching. The light of these "injection" pulses is polarized perpendicularly to and "incoherent" with the "background-" or "holding-" beam. Address pulses thus produce an injection of photocarriers, locally changing the optical properties of the resonator.

All observations are made within times lasting a few microseconds, repeated at 1 kHz, to eliminate thermal effects. Acousto-optic modulators (AOM) serve for fast intensity modulation of the injected optical fields, with a time resolution of 50 ns. They can be programmed to produce complex pulse-shapes, and to synchronize the drive and address pulses.

A variety of detection equipment is employed. A CCD camera records two-dimensional images, but with slow time response. Images are thus most useful for stable steady-state structures. Observations of intrapulse dynamics are done with a fast detector (2 ns), which monitors the incident power, and measures reflected light intensity with a spatial resolution of 4 μm . The good repeatability of the spatio-temporal dynamics allows to map the intensity dynamics on a diameter of the illuminated area, by successively imaging the points of the diameter onto the detector while recording the intensity

in each point as a function of time.

At large $\Delta\lambda$ and small negative $\delta\lambda$ ($|\delta\lambda| \leq 1$ HWHM) hexagonal structures form (Fig. 1). Hexagonal patterns appear in many different fields of physics [11], and have also been predicted, but not previously observed, for non-linear resonators [12,13]. The period of the hexagonal lattice is about $20 \mu\text{m}$, consistent with typical predictions for semiconductor models [13]. Our interpretation of Fig. 1 is that it is the result of a supercritical modulational instability of the unswitched branch. There is no observable threshold intensity for this pattern, however. We attribute this to a blurring of the threshold due to spatial and temporal variations and fluctuations of the input beam. Note that Fig. 1 is the reflected signal, so the imaged negative hexagons (lattice of dark spots) corresponds in terms of intracavity intensity to positive hexagons (lattice of bright spots).

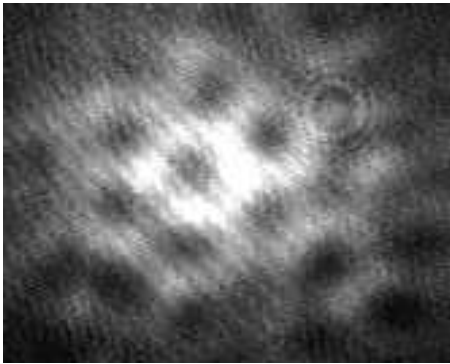


FIG. 1. Hexagonal pattern observed for the following parameters: $\Delta\lambda = 25 \text{ nm}$, $\delta\lambda = -1$ HWHM, power 30 mW , size of illuminated area $60 \mu\text{m}$.

The lattice period is measured to scale linearly with $1/\sqrt{\delta\lambda}$ as expected for tilted waves [12,14], which we expected to be the basic mechanism of this hexagon formation. We observe a change from negative to positive hexagons with decreasing $\delta\lambda$. The contrast of the pattern decreases with increasing $\delta\lambda$. Above $\delta\lambda = 1.5$ HWHM OB switching occurs before a pattern with notable contrast develops, when increasing the intensity. Since the illumination is with a Gaussian beam, the central part of the field switches first. The switched domain is separated from the surrounding unswitched area by a stationary switching front [15]. Such a switching front moves if the incident light intensity is different from the "Maxwellian" [15] intensity, the intensity for which the potential maxima for lower and upper branch are equally deep. The front moves into the unswitched area if the local incident intensity is larger than the Maxwellian intensity [15] and vice versa. It is stationary only on the contour on which the incident light intensity equals

the Maxwellian intensity. Thus switching fronts can be moved by changing the incident light intensity, as Fig. 2 shows.

Fig. 2a gives the incident and reflected intensity at the center of the Gaussian beam as a function of time; 2b and 2c show the intensity along a diameter of incident and reflected beam respectively as a function of time in the form of equiintensity contours. The recording Fig. 2d gives the reflectivity of the resonator along the same diameter of the Gaussian beam.

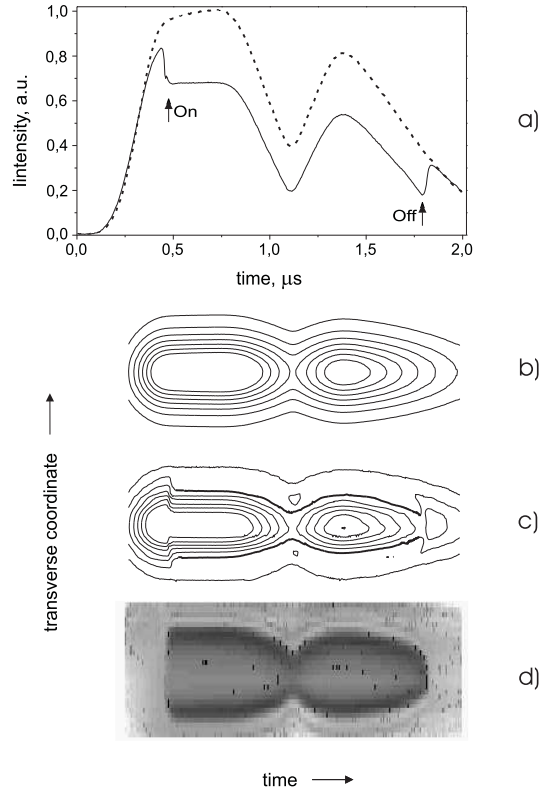


FIG. 2. Motion of switching front: a) incident light intensity (dashed) and light intensity reflected from sample, center of Gaussian beam (solid), b) intensity contours of incident light, c) intensity contours of reflected light (switching front matches the third lowest intensity contour of incident light), d) reflectivity of sample (darkest zones are the switching front).

Parameters are: $\Delta\lambda = 17 \text{ nm}$, $\delta\lambda = -1.6$ HWHM, power 70 mW , spot size $60 \mu\text{m}$.

Same time scale for a, b, c, d.

The light intensity is programmed here by the AOM as described above in order to study switching-wave dynamics. An initial peak (2a) switches most of the beam cross section to the low reflectivity state. During the rapid initial outward motion of the switching front (as well as the inward motion at switch-off) the position of the switching front is probably not adiabatically controlled by the

light field. As predicted [15], for adiabatic motion the switching front follows an intensity contour of the varying incident light; as evident by comparing 2b and 2c.

As opposed to the extended patterns (Fig. 1) localized structures (spatial cavity solitons) have been predicted [5,6]. Such structures can form due to interaction between switching fronts, in which context they have been called "diffractive autosolitons" [15].

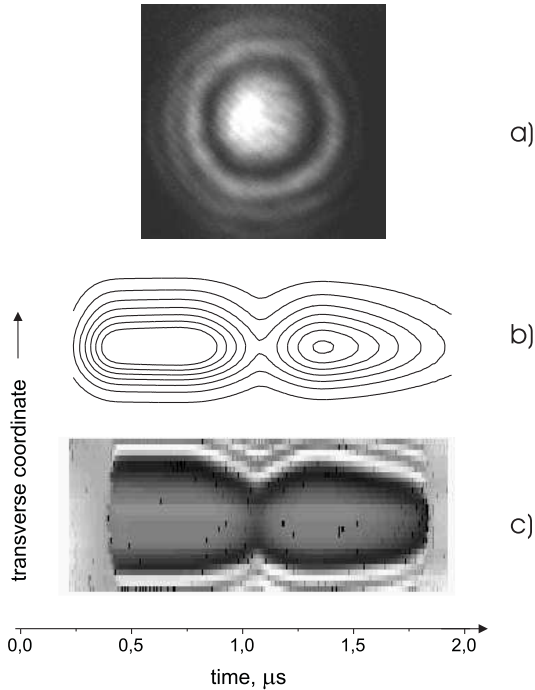


FIG. 3. Switching front with oscillating tails: a) switching front (darkest ring) surrounded by equidistant rings in unswitched area, b) intensity contours of incident light, c) reflectivity of sample. Parameters are: $\Delta\lambda = 25$ nm, $\delta\lambda = -1.6$ HWHM, power 80 mW, spot size $60\ \mu\text{m}$.

If switching fronts have "oscillating tails", the gradients associated with these oscillations can mutually trap two switching fronts. In 2D such "oscillating tails", which can occur due to a nearby modulational instability [16], may stabilize a circular switching front. This is equivalent to a localized structure or spatial soliton, which is free to move as a whole unless constrained by boundary effects. This mechanism of formation of such spatial solitons was studied theoretically [17] and demonstrated already experimentally [18] on a system with phase bistability. Oscillating tails are readily observable in the present system by choosing appropriate $\delta\lambda$ and $\Delta\lambda$; as seen in Fig. 3. Similar front-locking may thus occur in systems with intensity bistability such as the present one. The stabilization of front distances can thus be used as one criterion for the existence of spatial solitons. An-

other criterion is evidently the moveability of localized structures, which, furthermore, implies bistability of the structure.

Fig. 4 shows a corresponding observation. The intensity on a diameter of the illuminated field is recorded as a function of time. The background illumination is set in the middle of the bistability range.

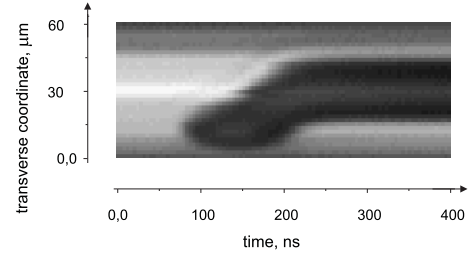


FIG. 4. Motion of switching front for off-center local switching. Parameters of the holding beam as in Fig. 3.

At some distance from the beam center a narrow ($8\ \mu\text{m}$) injection pulse can locally switch a small area to the upswitched branch. Fig. 4 shows how this switched spot moves to the center of the illuminated area (due to the intensity gradient of the background field). It would appear that the two points of the circular switching front, which can be followed in Fig. 4, move in parallel, suggesting a moving stable structure.

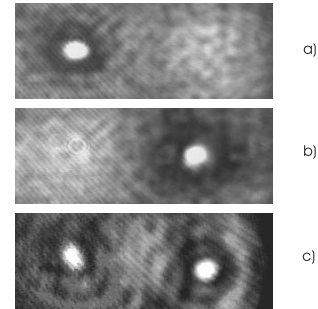


FIG. 5. Location of bright switched spot on two intensity maxima of the background field. Observation $400\ \mu\text{m}$ below sample surface (see text).

After the structure has reached the center of the field, where the intensity is maximal, it remains there stationarily. When there are two or more local intensity maxima in the background illumination, the final position of the up-switched structure can be at any of the maxima. Fig. 5 shows a background illumination, which has an intensity saddle at the center of the picture and local maxima at the center of the left and right half of the picture. Depending on whether the injection is (anywhere) in the right or the left half of the picture, the final position of

the up-switched structure will be the left or right intensity maximum respectively (Fig. 5a,b). Equally, at the two maxima up-switched structures can exist simultaneously (Fig. 5c).

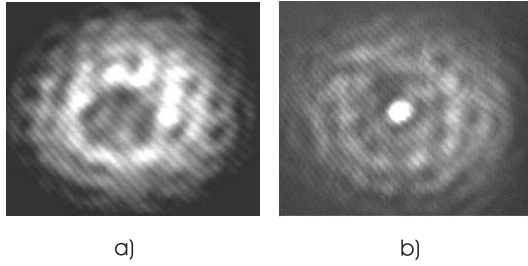


FIG. 6. Switched spot embedded in structured background. Observation on (a)) and 400 μm below (b)) sample surface.

Parameters are: $\Delta\lambda = 25 \text{ nm}$, $\delta\lambda = -1 \text{ HWHM}$ power 40 mW, spot size 60 μm .

At small $\delta\lambda$, when the background intensity is increased beyond the appearance of a high contrast hexagonal pattern a noticeably small spot ($\approx 10 \mu\text{m}$) appears as the switched-up structure, Fig. 6. For better measurement signal to noise ratio we have recorded in Figs 5 to 8 in a plane 400 μm below the sample surface. In this plane the structures appear bright, regular, with high contrast compared to the structures in the sample plane. Thus allowing to reduce the recording averaging times.

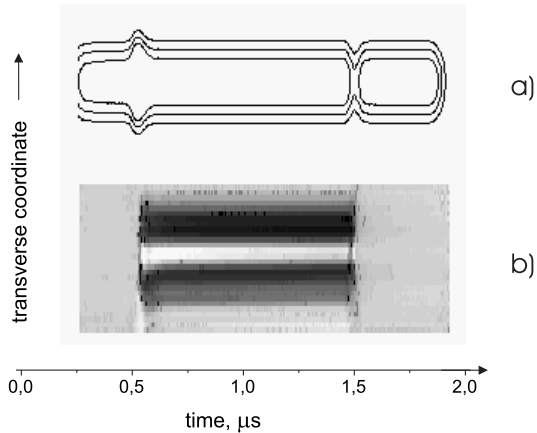


FIG. 7. Bistability of localized structure. a) intensity contours of incident light, b) reflectivity of sample.

Fast short increase of incident light intensity switches localized structure on. Fast short reduction of incident light intensity switches localized structure off.

Parameters as in Fig. 6.

Because of the small size and high brightness of the structure in Fig. 6b further tests were done on its soliton properties. The first test (bistability) is shown in Fig. 7.

Fig. 7a shows intensity contours of the incident light in the same way as Fig. 2b. Fig. 7b shows the light intensity reflected from the sample. The initial background intensity is chosen in the middle of the bistability range. A short (pulsed) increase of intensity (at ca. 0.5 μs) is then seen to switch the sample up. The small bright structure remains up-switched when the intensity is returned to its initial value below the switching limit. The small structure is switched back off by momentary decrease of the illumination to below the lower bistability limit (at ca. 1.5 μs). This is clear proof of bistability as expected for a spatial soliton.

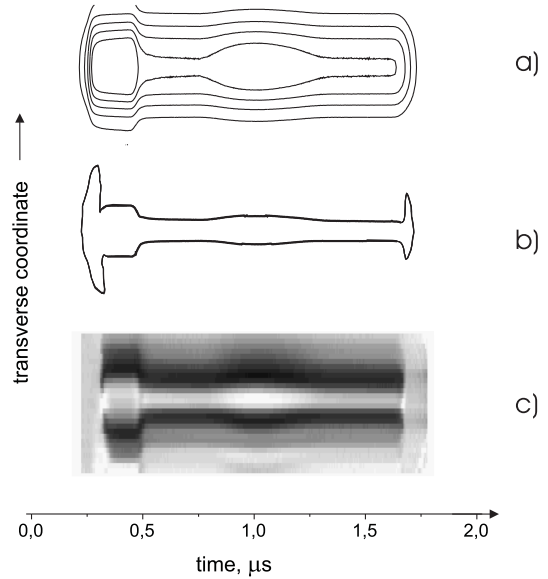


FIG. 8. Test of localized structure robustness. a) intensity contours of incident light, b) intensity contour of reflected light, c) reflectivity of sample.

Note that there is no intensity contour of the incident light which matches the contour of the bright zone.

Parameters as in Fig. 6.

If this structure is just a small up-switched domain, then the switching fronts surrounding it should follow an equintensity contour of the background field. If, on the other hand, there is "locking" of the switching front, it should not follow precisely the intensity changes. The result of the test is shown in Fig. 8: 8a and 8b give intensity contours for the incident and reflected light respectively, 8c gives the reflectivity. At the beginning the small structure is created by an initial pulse above the switching threshold, followed by a reduction of input intensity to a value in the middle of the bistability range. The test for robustness is then done by variation of the intensity (within the bistability range). Fig. 8b,c shows that the spatial variation of the reflected intensity, and thus of the switching front, is much less marked than that of the incident light intensity, in contrast to what

we observe in Fig. 2. This indicates a "robustness" of the structure indicative of self-localization.

Fig. 9 gives evidence that in hexagonal patterns the individual bright spots can have properties of localized structures or spatial solitons. 9a shows a hexagonal structure seemingly similar to Fig. 1. The intensity of the background field is in the middle of the bistability range. Injection with a narrow beam in a short pulse aimed at the bright spot marked "a" in 6a, switches it, as seen in 9b, to be a dark "defect". When the injection beam is aimed at the adjacent spot (marked "b"), this adjacent spot is switched off, all other spots remaining unchanged. To demonstrate that the switched spot is stable, we show in Fig. 9d the output from that region as a function of time during the $2\ \mu\text{s}$ duration of the main input pulse. In the upper trace, the address pulse is too weak to induce switching, and the output recovers within 100ns to its original steady value. In the lower trace, switching does occur, and the output remains almost constant at a level less than 20 % below its original value, until the holding light is returned to zero. Thus unlike a coherent extended hexagon pattern, the structure of Fig. 9a behaves like a collection of localized structures, who can independently be switched.

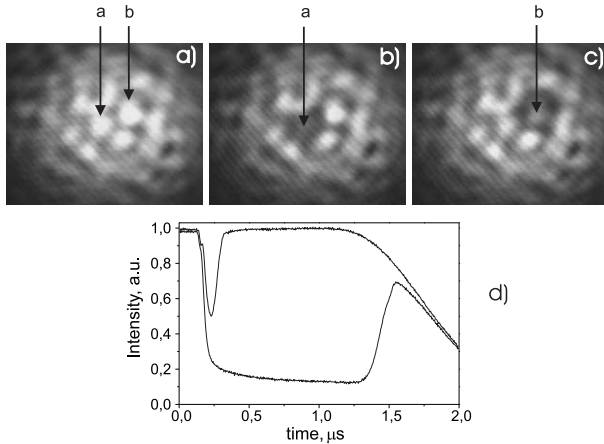


FIG. 9. Switching of individual bright spots of a bright spot cluster (see text). Parameters are: $\Delta\lambda = 25\ \text{nm}$, $\delta\lambda = -1\ \text{HWHM}$, holding beam width $60\ \mu\text{m}$, injecting beam width $8\ \mu\text{m}$.

Concluding, we have shown for the first time the formation of hexagon patterns, as predicted for non-linear passive resonators. Evidence was given of soliton properties of small spatial structures.

Acknowledgements

This work was supported by ESPRIT LTR project PI-ANOS. Discussions with the project partners are acknowledged. We thank W.J.Firth for valuable suggestions. We also thank K.Staliunas for developing clarifying

concepts such as the linear filtering of spatial noise by a 2D resonator.

-
- [1] L.A.Lugiato, M.Brambilla, A.Gatti, *Advances in Atomic, Molecular, and Optical Physics* **40**, 229 (1999).
 - [2] C.O.Weiss, M.Vaupel, K.Staliunas, G.Slekys, V.B.Taranenko, *Appl. Phys. B* **68**, 151 (1999).
 - [3] K.Staliunas, *Phys. Rev. A* **48**, 1573 (1993).
 - [4] C.O.Weiss, H.R.Telle, K.Staliunas, M.Brambilla, *Phys. Rev. A* **47**, R1616 (1993); M.Vaupel, C.O.Weiss, *Phys. Rev. A* **51**, 4078 (1995); M.Vaupel, K.Staliunas, C.O.Weiss, *Phys. Rev. A* **54**, 880 (1996).
 - [5] M.Tlidi, P.Mandel, R.Lefever, *Phys. Rev. Lett.* **73**, 640 (1994).
 - [6] W.J.Firth, A.J.Scroggie, *Phys. Rev. Lett.* **76**, 1623 (1996); M.Brambilla, L.A.Lugiato, F.Prati, L.Spinelli, W.J.Firth, *Phys. Rev. Lett.* **79**, 2042 (1997).
 - [7] M.Kreuzer, W.Balzer, T.Tschudi, *Appl. Opt.* **29**, 579 (1990); M.Kreuzer, H.Gottschling, T.Tschudi, R.Neubecker, *Mol. Cryst. Liq. Cryst.* **207**, 219 (1991); J.Nalik, L.M.Hoffer, G.L.Lippi, Ch.Vorgerd, W.Lange, *Phys. Rev. A* **45**, R4237 (1992).
 - [8] L.A.Lugiato, R.Lefever, *Phys. Rev. Lett.* **58**, 2209 (1987).
 - [9] S.Coen, M.Haelterman, *Opt. Lett.* **24**, 80 (1999).
 - [10] B.G.Sfez, J.L.Oudar, J.C.Michel, R.Kuszelewicz, R.Azoulay, *Appl. Phys. Lett.* **57**, 1849 (1990); I.Abram, S.Iung, R.Kuszelewicz, G.LeRoux, C.Licoppe, J.L.Oudar, *Appl. Phys. Lett.* **65**, 2516 (1994).
 - [11] G.Dewel, S.Mtens, M'F.Hilaly, P.Borckmans, C.B.Price, *Phys. Rev. Lett.* **74**, 4647 (1995).
 - [12] W.J.Firth, A.J.Scroggie, *Europhys.Lett.* **26**, 521 (1994).
 - [13] L.Spinelli, G.Tissoni, M.Brambilla, F.Prati, L.A.Lugiato, *Phys. Rev. A* **58**, 2542 (1998); D.Michaelis, U.Peschel, F.Lederer, *Phys. Rev. A* **56**, R3366 (1997).
 - [14] P.V.Jakobsen, J.V.Moloney, A.C.Newell, R.Indik, *Phys. Rev. A* **45**, 129 (1992).
 - [15] N.N.Rosanov, 1996 *PROGRESS in OPTICS* **35**, 1 Ed. E.Wolf
 - [16] N.N.Rosanov, G.V.Khodova, *JOSA B* **7**, 1057 (1990).
 - [17] K.Staliunas, V.J.Sanchez Morcillo, *Phys. Rev. A* **57**, 1454 (1998); K.Staliunas, V.J.Sanchez-Morcillo, *Phys. Lett A* **241**, 28 (1998).
 - [18] V.B.Taranenko, K.Staliunas, C.O.Weiss, *Phys. Rev. Lett.* **81**, 2236 (1998); V.B.Taranenko, M.Zander, P.Wobben, C.O.Weiss, *Appl. Phys. B* **69** 337 (1999).